Title

Enhancing protein disulfide bond cleavage by UV excitation and electron capture dissociation for top-down mass spectrometry

Authors

Wongkongkathep, Piriya
Li, Huilin
Zhang, Xing
et al.

Publication Date

2015-11-01

DOI

10.1016/j.ijms.2015.07.008

Peer reviewed

HHS Public Access

Author manuscript

Int J Mass Spectrom. Author manuscript; available in PMC 2016 November 15.

Published in final edited form as:

Int J Mass Spectrom. 2015 November 15; 390: 137–145. doi:10.1016/j.ijms.2015.07.008.

Enhancing Protein Disulfide Bond Cleavage by UV Excitation and Electron Capture Dissociation for Top-Down Mass Spectrometry

Piriya Wongkongkathep[1], **Huilin Li**[2], **Xing Zhang**[4], **Rachel R. Ogorzalek Loo**[2], **Ryan R. Julian**[4], and **Joseph A. Loo**[1,2,3,*]

[1]Department of Chemistry and Biochemistry, University of California-Los Angeles Los Angeles, CA 90095

[2]Department of Biological Chemistry, University of California-Los Angeles Los Angeles, CA 90095

[3]UCLA/DOE Institute of Genomics and Proteomics, University of California-Los Angeles Los Angeles, CA 90095

[4]Department of Chemistry, University of California-Riverside, Riverside, CA 92521

Abstract

The application of ion pre-activation with 266 nm ultraviolet (UV) laser irradiation combined with electron capture dissociation (ECD) is demonstrated to enhance top-down mass spectrometry sequence coverage of disulfide bond containing proteins. UV-based activation can homolytically cleave a disulfide bond to yield two separated thiol radicals. Activated ECD experiments of insulin and ribonuclease A containing three and four disulfide bonds, respectively, were performed. UV-activation in combination with ECD allowed the three disulfide bonds of insulin to be cleaved and the overall sequence coverage to be increased. For the larger sized ribonuclease A with four disulfide bonds, irradiation from an infrared laser (10.6 μm) to disrupt non-covalent interactions was combined with UV-activation to facilitate the cleavage of up to three disulfide bonds. Preferences for disulfide bond cleavage are dependent on protein structure and sequence. Disulfide bonds can reform if the generated radicals remain in close proximity. By varying the time delay between the UV-activation and the ECD events, it was determined that disulfide bonds reform within 10–100 msec after their UV-homolytic cleavage.

Graphical abstract

*Corresponding author at: University of California-Los Angeles, Department of Chemistry and Biochemistry, 402 Boyer Hall, Molecular Biology Institute, Los Angeles, CA, United States, Tel.: +1 310 794 7023; fax: +1 310 206 4038, JLoo@chem.ucla.edu (J.A. Loo).

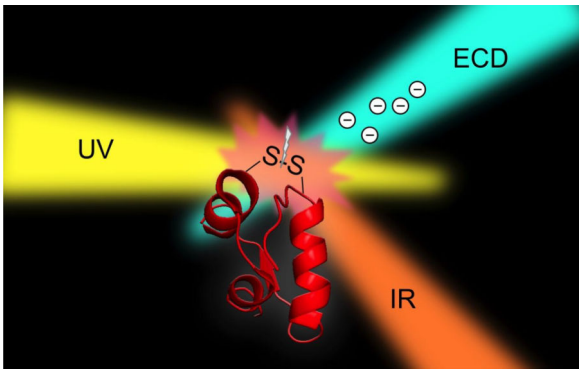

1. Introduction

Disulfide bonds are one of the most important post-translational modifications because they aid proteins to preserve their tertiary structure [1, 2]. The development of methods for the structural elucidation of protein disulfide bonds has been on-going for many years. As antibodies and antibody-drug conjugates become more popular in the market as therapeutic drugs, the development of efficient, rapid, and accurate methods for characterizing disulfide bond linkages become more important [3, 4].

Several mass spectrometry approaches for characterizing disulfide bonds have been reported in the literature [5, 6]. A common strategy employs chemical reduction of the S-S bond (with, for example, dithiothreitol or TCEP (*tris*(2-carboxyethyl)phosphine)), followed by alkylation of the free thiols to prevent disulfide scrambling; the resulting protein is digested with a suitable protease and the peptide products are measured by LC-MS/MS. However, information of the disulfide bond linkages (i.e., residues) can be lost [5]. In some cases, partial reduction and alkylation can be used, but this results in complex mixtures of peptides with differing amounts of alkylated residues [7]. Top-down MS analysis, i.e., direct analysis and dissociation of the intact gas phase protein without prior chemical/enzymatic fragmentation into smaller peptides, has been considered because it skips the time-consuming proteolysis and chromatographic separation steps [8, 9]. The number of disulfide bonds can be directly by determined from an accurate intact protein mass measurement and comparison to the theoretical sequence mass. However, top-down analysis of disulfide bonded proteins remains challenging due to the limited efficiency of disulfide bond fragmentation. Backbone fragments often still remain connected by S-S bridges and it becomes difficult to interpret the product ion mass spectra to obtain sequence information within disulfide-bridged regions [10–12].

More than a decade ago, McLafferty's group introduced the development and application of electron capture dissociation (ECD) with MS for protein sequencing [13, 14]. The early ECD-MS work demonstrated its capability to not only cleave backbone bonds for large proteins, but also disulfide bonds for peptides [15], while leaving labile post-translational modifications and non-covalent interactions intact. Possible mechanisms of ECD related to disulfide bonds include the migration of a hydrogen radical ($H^{\bullet}$) from a neutralized ammonium group at an electron capture site to a disulfide bond to form $-S^{\bullet}$ and –SH

(Cornell mechanism), or another possibility is that an S-S bond captures an electron to generate $–S^{\bullet}$ and $–S^{-}$, which is converted to –SH later (Utah-Washington mechanism) [16–18]. Electron transfer dissociation (ETD) [19] has also shown some capabilities for disulfide bond cleavage [20, 21]. However, the efficiency for disulfide bond cleavage for *proteins* is relatively low, even with additional collisional and vibrational excitation [22].

There have been several alternative techniques proposed to cleave disulfide bonds for characterization by top-down MS. These include online electrolytic reduction prior to electrospray [23–26], activation/dissociation of metal cation-adducted species [27], and radical-driven approaches [28]. Our research group previously introduced supercharging reagents to enhance charging of native proteins and complexes [29–31]. We demonstrated that by activating higher charged proteins, ECD could access more sequence information, especially for proteins containing multiple disulfide bonds [32].

Laser-based approaches have also been tested to tackle this problem. Because the maximum absorption of a disulfide bond is in the vacuum-UV region (around 150 nm for cystine [33]), 157-nm ultraviolet photodissociation (UVPD) was used to target disulfide bond cleavage; however, some competitive dissociation channels of protein backbone were observed [34]. Julian's group demonstrated the use of 266 nm UVPD to provide more selective disulfide bond cleavage in peptides [35]; this work was based on a possible mechanism that utilized electronic energy transfer (EET) from neighboring tyrosine or tryptophan residues [36]. However, there remains the question on whether any of these methods can be applied to larger molecules such as proteins. In this work, we demonstrate that 266 nm UVPD could be combined with vibrational excitation through infrared laser activation to give rise to backbone cleavage for small proteins, and we show evidence that suggests a strong relationship between disulfide bond cleavage and EET via an adjacent tyrosine residues.

2. Experimental

2.1. Materials

Two disulfide bond-containing proteins, bovine insulin (UniprotKB P01317) and bovine ribonuclease A (UniprotKB P61823) were purchased from Sigma-Aldrich (St. Louis, MO). The proteins were resuspended in water and desalted by centrifugal filtration using 3 kDa MW cutoff (MWCO) membranes for insulin and 10 kDa MWCO for ribonuclease A. The desalted proteins were dissolved in 50:50:0.1 (*v/v/v*) H_2O/CH_3CN/formic acid.

2.2. Instrumentation

A 15-Tesla SolariX FT-ICR mass spectrometer equipped with an infinity cell (Bruker Daltonics, Bremen, Germany) was used for the high-resolution top-down MS experiments. Two types of lasers were used for the experiments. A 10.6 μm (30 W) infrared beam was generated by a CO_2 laser (Synrad, Mukilteo, WA). UV radiation (266 nm) was generated from the 4^{th} harmonic of a Nd:YAG laser (Continuum, Santa Clara, CA). A BaF_2 window was mounted on the end flange of the vacuum system to allow the unfocussed laser beams to pass through to the infinity ICR cell. A fused-silica window beamsplitter (Esco Optics, Oak Ridge, NJ) was aligned 45° to both the infinity cell and the 10.6 μm IR beam, acting to

reflect the IR beam partially while transmitting the 266 nm UV beam (Figure 1). Because the UV and IR laser beams propagated to the center of the infinity cell overlapped and were co-linearly aligned, UV and IR irradiation can be applied individually or together without realignment. Both lasers were triggered by unique TTL pulses from the FT-ICR mass spectrometer data system, controlled by a customizable pulse program. An iodinated-tyrosine containing peptide (*N-4*-iodobenzoyl-RGYALG) was used to test the alignment of the UV laser by generating the [RGYALG]$^{\bullet}$ radical from homolytic C–I bond cleavage [37].

2.3. Mass spectrometry and MS/MS analysis

Samples were directly infused into the FT-ICR mass spectrometer by nanoelectrospray ionization (nanoESI) using Au/Pd coated borosilicate emitters (Thermo Scientific, San Jose, CA). The ESI voltage was set to 800–1000 V. The instrument parameters were set to the following: glass transfer capillary temperature, 180 °C; applied voltages to ion funnel and skimmer were 120 and 50 V, respectively; ion source RF frequency was set to 200 V_{pp}; quadrupole and hexapole RF frequencies were 2 MHz, 1200 V_{pp}. Ions were accumulated for 0.5 sec before sending them to the ICR cell with the time-of-flight of 1.2 msec. The signal transient length was set to 2.8 sec to achieve a resolving power of 800,000 at *m/z* 400. The isolation power was to 35%. Precursor ions were isolated by the quadrupole and transferred into the ICR cell to perform ECD or activated-ion ECD (activation by UV or IR irradiation or both). The electron energy for ECD was 1 eV (10 ms pulse and 15 V on the lens). ECD fragments were detected by the SNAP centroid peak detection algorithm (Bruker Daltonics) and manually assigned against theoretical fragments obtained from Protein Prospector. Mass spectra were externally calibrated with CsI.

3. Results and Discussion

3.1. Structural overview

Insulin consists of two peptide chains (chain A: 21 residues, and chain B: 30 residues). It is first synthesized in beta cells as a single chain, proinsulin. After being processed by proteases, cleaving off the C-peptide in the middle of its sequence, it becomes mature insulin [38]. Two intermolecular disulfide bonds connect chain A and B: $C7_A$-$C7_B$, $C20_A$-$C19_B$. There is another intramolecular disulfide bond linking C6 and C11 on chain A. Ribonuclease A (RNaseA; bovine) is a small 13.7 kDa single-chain protein that has a complex intramolecular linkage, containing four disulfide bonds. The amino acid sequences of insulin and ribonuclease A are shown in Figure 2.

The ESI mass spectrum of denatured insulin shows a narrow charge state distribution from 6+ to 4+. The mass spectrum of denatured RNaseA showed relatively low charging from 12+ to 5+ compared to the disulfide-reduced form [39–41], with the maximum intensity measured for the 8+ charged molecule. Disulfide bonds prevent the protein to be completely unfolded and fully protonated to yield maximum charging (Figure 3).

3.2. UV irradiation separates insulin chains and preferentially fragments RNaseA

To study how 266 nm UV activation affects protein fragmentation, a series of short pulses (~8 nsec, 4 mJ per pulse) was fired and directed into the ICR cell where ions were trapped.

Disulfide bond cleavage by photodissociation was readily observed when 10 laser shots per spectra were applied. For insulin, ions for both chains A and B were detected, confirming that the two intermolecular disulfide bonds were cleaved by PD and yielded a separation of both A and B chains (Figure 4a). The measured masses of both chains confirmed that homolytic cleavage (—S• •S—) occurred. However, the PD yield was low; relative abundances for the liberated chains A and B were only 1% relative to the precursor ion abundance. This result might be expected because both intermolecular disulfide bonds need to be cleaved to separate the two chains. A number of y-product ions from the C-terminal portion of the B-chain outside of the disulfide bonds were observed, such as $y_{4,B}$, $y_{5,B}$, and $y_{6,B}$ (where the "B" denotes that it originates from chain B), in addition to b-fragments from chain B connected to intact chain A (e.g., $b_{24,B}$+A, $b_{25,B}$+A, $b_{26,B}$+A). The observed collisionally activated dissociation (CAD)-type ions (i.e., b/y) can occur following internal conversion of the photon energy into vibrational excitation and should yield fragments similar to what is observed by CAD or IRMPD.

For RNaseA, there was no direct evidence of disulfide bond cleavage from only PD because the protein mass remains the same after homolytic cleavage(s) of the disulfide bond(s). Interestingly, cleavage of a bond between Val_{116}-Pro_{117} to generate the y_8 ion ($PVHFDASV_{124}$) was found for PD of the $[M+11H]^{11+}$ molecule (Figure 4b). This may suggest that UV irradiation was absorbed by the protein probably from a nearby tyrosine (Tyr-115). Formation of the y_8 ion was likely from UV photoactivation resulting in an elevated internal energy to produce a favorable cleavage at the proline residue [42, 43]. The abundance of the y_8 ion was about 2% relative to the precursor. The complimentary ion, $[M-y_8+10H]^{10+}$, was observed also, in addition to charge stripped $[M+10H]^{10+}$ and $[M-y8+9H]^{9+}$. From this evidence for insulin and ribonuclease A, 266 nm irradiation can photodissociate and photoactivate small proteins, but the PD yields are relatively low.

3.3. Disulfide bond cleavage of insulin by UV-enhanced ECD

Although ECD alone can cleave disulfide bonds for disulfide-linked peptides, the efficiency is low for proteins and it may be sequence dependent [22]. In some cases, such as 20 kDa trypsin inhibitor, ECD does not promote disulfide bond cleavage. In our study, UV activation combined with ECD was aimed to enhance disulfide bond cleavage. Insulin and RNaseA were tested with ECD alone, and with some pre-activation by UV and IR irradiation. Backbone cleavage of regions enclosed by disulfide bonds will be indicative of the presence of disulfide links.

The 6+ charge state, which was the highest charge observed for insulin, was isolated and transferred into the ICR cell to perform ECD or UV-activated ECD. ECD mass spectra were acquired from an average of 200 microscans. Upon ECD, two charge-reduced species ($[M+6H]^{5+\bullet}$ and $[M+6H]^{4+\bullet\bullet}$) were observed. Small c/z$^{\bullet}$-type fragments were observed between *m/z* 400–1000 (e.g., $c_{5,A}$, $c_{4,B}$, $c_{6,B}$, $z_{8,B}$, $z_{9,B}$). Larger fragments linked to one of the intact chains were detected at *m/z* 1200–1800 (for instance, $c_{23,B}$+A, $c_{28,B}$+A, $z_{27,B}$+A, $z_{29,B}$+A, $c_{20,A}$+B, $z_{16,A}$+B, $z_{26,A}$+B). However, the majority of the fragments were from outside both intermolecular disulfide bonds ($C7_A$-$C7_B$, $C20_A$-$C19_B$). Also observed were b/y-type product ions ($b_{4,A}$, $y_{4,B}$, $y_{6,B}$, $y_{7,B}$, $y_{8,B}$, $y_{9,B}$, and $y_{20,A}$+B). Figure 5 summarize the

backbone cleavage coverage of ECD of the insulin 6+ charge state. Interestingly, six fragments showed evidence of intermolecular disulfide bond cleavage of $C20_A$-$C19_B$: $z_{13,B}$, $z_{15,B}$, $z_{16,B}$, $c_{14,B}$+A, $c_{19,B}$+A, and $c_{17,A}$+B (Figure 6a). The ECD results are consistent with previous reports by McLafferty, McLuckey, and Breuker [15, 22, 44]. The loss of S and •SH was observed, which is also an indication of disulfide bond cleavage. From the c/z$^{\bullet}$-fragments when only ECD was applied, only one disulfide bond ($C20_A$-$C19_B$) was cleaved, and the other two S-S bonds remained intact. Overall, 51 product ions were observed and cleavage of 51% of the total possible inter-residue linkages was achieved.

For UV-assisted ECD, 10-pulses of the UV laser were programmed to fire immediately prior to ECD, with no additional time delay between the UV laser and ECD events. From the results, it is clear that UV activation improved the ECD efficiency for disulfide bond cleavage. The total number of backbone cleavages increased slightly from 51 to 68, but most of the new products (15) were from regions within the formerly disulfide bond-enclosed area. These newly created fragments were not observed with ECD alone. The fragmentation pattern indicated that all three disulfide bonds were cleaved. Similar to ECD alone, products $z_{13,B}$, $z_{15,B}$, $z_{16,B}$, $c_{14,B}$+A, and $c_{19,B}$+A indicated dissociation of the intermolecular $C20_A$-$C19_B$ bond (Figure 6b). Evidence for $C7_A$-$C7_B$ bond dissociation is given by product ions $c_{8,A}$, $c_{11,A}$, $c_{14,A}$, $c_{16,A}$, $c_{8,B}$, $c_{9,B}$, $c_{12,B}$, $c_{13,B}$, $y_{22,B}$+A, and $z_{4,A}$+B. The $c_{8,A}$ ion confirmed that the $C6_A$-$C11_A$ disulfide bond was cleaved. Moreover, some fragments ($c_{25,B}$ and $c_{29,B}$) suggested (near) simultaneous cleavage of both intermolecular disulfide bonds to yield the separation of chains A and B, as found for UVPD alone (*vide supra*). Upon UV photoactivation prior to ECD, 73% of the total possible inter-residue linkages were cleaved. Out of the 68 total fragments observed, 31% (21) originated within the formerly disulfide bonded regions.

Disulfide bond cleavage efficiency was further quantified as the relative abundance of the disulfide bond derived fragments (%SS abundance) as defined by:

$$\%SS abundance = \frac{\Sigma production\ intensity\ from\ disulfide\ bridged\ region}{\text{total production intensity observed}} \quad \text{Equation 1}$$

The %SS abundance increased from 1.6% for ECD alone to 8.1% for UV activation/ECD, indicating the significant improvement of using UV pre-activation for ECD of disulfide bonds for insulin.

3.4. UV with vibrational excitation can assist ECD to cleave RNaseA disulfide bonds

Ribonuclease A has four intramolecular disulfide bonds (C26–C80, C40–C95, C58–C110, and C65–C72) that predominantly cover residues 26–110, which represent 68.5% of the protein sequence (Figure 2). The $[M+11H]^{11+}$ and $[M+10H]^{10+}$ molecules were chosen for the ECD and UV-activated ECD experiments. The c/z$^{\bullet}$-ion abundances were normalized and displayed against each cleavage site; the eight cysteine residues that form the four intramolecular disulfide bridges are displayed as vertical lines in the fragmentation plots (Figure 7).

ECD of RNaseA yielded c/z•-fragments that were solely from the regions that are not bridged by disulfide bonds, toward the N- and C-terminal ends (i.e., $c_{2–24}$, c_{121}, c_{122}; z_6, z_9, z_{12}, z_{121}' and z_{122}'). Increasing collisional activation prior to ECD by increasing the skimmer voltage to 60 V, as suggested by Ganisl and Breuker [22], did not yield fragments in the disulfide-bridged region. We also implemented an additional vibrational excitation by IR laser irradiation prior to the ECD event, generally known as activated ion ECD (ai-ECD), to disrupt weak noncovalent interactions such as hydrogen bonds that may be holding c-/z-product pairs together [45] and can significantly improve ECD fragmentation efficiency [46–48]. Elevated internal energy from IR irradiation also enhances secondary ECD fragmentation that may play a role in disulfide bond cleavages. In this experiment, the ai-ECD of RNaseA generated four c-fragments from residues 33–36, which are in the region covered by the first disulfide bond (C26–C84), but not in the second (C40–C95) (Figure 7b). Three of the fragments, $c_{34–36}$, contained an extra hydrogen atom suggesting that the disulfide bond cleavage mechanism is from ECD and hydrogen radical migration.

Activated ion-ECD yielded only a single disulfide bond cleavage event in RNaseA, and so we investigated additional activation methods to facilitate disulfide bond cleavage from ECD radical cascade reactions. UV-activation prior to the ECD event was tested. Ten consecutive UV pulses were used without significantly reducing precursor signal intensity. Similar to ai-ECD, some fragments from residues 26–38 were observed (Figure 7c), indicating a single disulfide bond (C26–C84) was cleaved. Fragmentation from the disulfide-bridged region was slightly improved compared to ai-ECD; five newly-observed c-fragments (c_{26}+H, c_{27}+H, c_{30}+H, c_{32}+H, and c_{38}+H) were observed by UV-ECD. A total of 9 c-type ions out of 15 possible backbone cleavage sites between the first and second disulfide bonds (residues 26–39) were observed. However, the overall normalized abundance of fragments from the C26–C84 bridge region was low, around 5% relative to small fragments from the N-terminal region. The large number of small N-terminal fragments might indicate a secondary dissociation from secondary electron capture of larger fragments because most disulfide bonds were still intact. Along the C-terminal region outside the disulfide bridges, more c/z•-fragments were observed with higher abundance when UV-ECD was used.

To further improve the prospects for top-down protein disulfide bond cleavage, we utilized both UV- and IR-based activation prior to ECD by firing 10-shots of UV light followed by a 60-msec IR pulse. Because both UV and IR irradiation were used, the IR laser irradiation time was reduced from 120–150 msec (for normal ai-ECD experiments) to 60 msec to minimize CAD-type fragmentation prior to electron capture. Figure 8 shows the ECD-MS spectra with UV followed by IR activation (UV/IR) compared to ECD alone. Several new fragments were detected between *m/z* 1000–1500 from UV/IR-activated ECD. In the region of residues 26–39 that is covered by the first disulfide bond, 13 out of 14 available backbone cleavages (93%) were detected. Interestingly, c_{44}+2H and c_{45}+2H fragments were observed (Figure 7d), which results from cleavage of ***both*** the first (C26–C84) and second (C40–C95) disulfide bonds. Unlike fragments from the region between residues 26–39, the cleavage at sites 44 and 45 contains additional two hydrogen atoms, which is evidence for breaking two disulfide bonds. Moreover, the detection of z_{21} and z_{24} fragments confirmed that the third

disulfide bond (C58–C110) was cleaved (but only one disulfide bond cleavage is required to observe these fragments). Three representative ECD-type fragments, which indicated cleavage of the first, second, and third disulfide bonds, are shown in the mass spectra depicted in Figure 9. The loss of S and •SH, which is evidence of disulfide bond cleavage, was observed when UV was used and was more abundant when both UV- and IR-activation were applied. Overall, using both UV- followed by IR-activation provided the best results for RNaseA disulfide bond cleavage. The %SS abundance results are summarized in Figure 10a.

Further, the effects of reversing the chronological order of the two laser irradiation events prior to ECD was investigated (Figure 10b). With the IR excitation event immediately before UV-activation (IR/UV), the %SS abundance was slightly lower compared to UV/IR, but still higher than both single laser activation experiments (i.e., ai-ECD, UV-ECD). We considered that the radicals from UV homolytic cleavage could recombine if the two cysteine residues are in close proximity. Application of IR heating immediately after UV excitation could allow for the separation of the two thiol radicals immediately after their generation. IR activation mitigated disulfide bond reformation by reducing intramolecular noncovalent interactions. UV/IR-activation yielded more ECD fragmentation from the disulfide-bridged regions than the IR/UV approach.

We further investigated the kinetics of disulfide bond reformation. A short time delay was set between the UV laser (both 5 and 10 shots) and the ECD event with no additional vibrational activation applied (i.e., UV-ECD). The purpose of this experiment was to estimate the timescale of radical reformation. The delay ranged from 10 msec to 1 sec. The results (Figure 10b) showed that number of fragments from disulfide-bridged regions dropped significantly even with a 10 msec delay. Disulfide bond cleavage was no longer observed with a delay of longer than 100 msec, suggesting that the timescale of disulfide bond reformation was between 10–100 msec. The %SS abundance decayed slower with the greater number of UV laser shots (10) because more radicals from homolytic cleavage were generated.

Studies of small molecule disulfides, including dimethyl disulfide, diethyl disulfide, and 1,2-dithiane showed the dependence of S-S bond cleavage upon UV irradiation [49–51]. For straight chain diethyl disulfide, 266 nm photons lie at the red edge of the S1 absorption band, an excited state yielding S-S dissociation and radical formation on an ultrafast timescale, 30 ± 15 femtoseconds. For cyclic 1,2-dithiane, UV excitation was also found to cleave the disulfide on a sub-100 femtosecond timescale, but the diradical –S• ends oscillated around the excited state minimum, confined structurally. At certain distances, these –S• ends sampled regions where the S0 (ground) and S1 electronic states overlapped, resulting in ultrafast repopulation of the ground state (intact S-S bond). Hence, for cyclic or structurally restrained systems such as proteins, coupling between the S0 and S1 electronic states ensures that disulfides can rapidly cycle between cleaving and forming, until energy dissipates from the coupled modes. Hence, it is reasonable that the time dependence of productive photoexcitation/ECD is essentially that for radiative cooling.

Disulfide bonds can be cleaved by UV activation prior to ECD, but why are some bonds preferentially cleaved compared to others? The 266 nm wavelength of the UV laser used is close to a one-photon absorption band for aromatic residues like tyrosine and tryptophan. Disulfide bonds also absorb in this region, but more weakly than the aromatic residues [36, 52]. Julian's group described that energy absorbed by aromatic residues can be transferred to nearby cysteine residues by excitation energy transfer (EET) and it is strictly distance dependent [36]. Tryptophan has a working range of around 15 Å to facilitate disulfide bond cleavage, whereas tyrosine requires a shorter distance of less than 6 Å. Another report suggested that 270–290 nm UV excitation of tryptophan residues in solution is followed by transfer of electrons to the S-S bonds, resulting in their reduction, confirming the importance of tryptophan and tyrosine residues [53]. Insulin has no tryptophans, but $Y19_A$ is next to the $C20_A$ of the $C20_A$-$C19_B$ disulfide bond. Interestingly, fragments from $C20_A$-$C19_B$ cleavage exhibited higher signal intensities compared to other disulfide bond cleavages, and thus suggesting that the $C20_A$-$C19_B$ bond is the first disulfide bond that is preferentially cleaved by UV-ECD. The C26–C84 disulfide bond of RNaseA is preferentially cleaved by UV-ECD and UV/IR-ECD; C26 is adjacent to Y25. The second disulfide bond (C40–C95) is in close proximity to Y97, where the distance is two residues apart. Unfortunately, the efficiency of EET would be much lower, resulting in no fragments observed between sites 40–57 when only UV activation was used. Fewer fragments were observed when IR was combined with UV activation. Although C65–C72 is next to Y73, evidence for disulfide bond cleavage was not observed because the C65–C72 bridge is located in the middle of the sequence that is covered by the other three disulfide bonds. The single C65–C72 disulfide bond and some N-C_α bonds might be cleaved, but the fragments likely remained bound to the protein. All four disulfide bonds must be cleaved in order to separate the ECD fragments within C65–C72 region. Overall our results are in agreement with the EET model described previously.

4. Conclusion

Two separate laser systems, a UV laser operating at 266 nm in combination with an IR laser was interfaced to an FT-ICR mass spectrometer for promoting disulfide bond dissociation of gas phase proteins. UVPD was able to initiate homolytic cleavage of disulfide bonds as indicated by chain separation of insulin. With ECD only, one intermolecular disulfide bond can be cleaved. With UV pre-activation prior to ECD, all three disulfide bonds of insulin were cleaved. For ribonuclease A, none of the four intramolecular disulfide bonds could be cleaved by ECD alone. A significant improvement was shown by applying 10 shots of UV irradiation followed by vibrational activation before electron capture to cleave up to three disulfide bonds. Preferential bond cleavage is strongly affected by the sequence of the protein. For insulin and ribonuclease A, tyrosine appears to facilitate disulfide bond cleavage by EET if in a close proximity. In summary, we have demonstrated that UV excitation can enhance disulfide bond cleavage of intermolecular disulfide linked proteins and this method should be beneficial for protein characterization by top-down MS approaches.

Acknowledgments

Support from the US National Institutes of Health (R21GM103531, R01GM103479, S10RR028893), the US Department of Energy Office of Science, Office of Biological and Environmental Research program (UCLA/DOE Institute for Genomics and Proteomics; Award Number DE-FC02-02ER63421), and the Development and Promotion of Science and Technology Talents Project (DPST), Royal Thai Government (to P.W.) are acknowledged.

References

1. Wedemeyer WJ, Welker E, Narayan M, Scheraga HA. Disulfide Bonds and Protein Folding. Biochemistry. 2000; 39:4207–4216. [PubMed: 10757967]
2. Matsumura M, Signor G, Matthews BW. Substantial increase of protein stability by multiple disulphide bonds. Nature. 1989; 342:291–293. [PubMed: 2812028]
3. Wypych J, Li M, Guo A, Zhang Z, Martinez T, Allen MJ, Fodor S, Kelner DN, Flynn GC, Liu YD, Bondarenko PV, Ricci MS, Dillon TM, Balland A. Human IgG2 Antibodies Display Disulfide-mediated Structural Isoforms. J. Biol. Chem. 2008; 283:16194–16205. [PubMed: 18339624]
4. Zhang W, Marzilli LA, Rouse JC, Czupryn MJ. Complete disulfide bond assignment of a recombinant immunoglobulin G4 monoclonal antibody. Anal. Biochem. 2002; 311:1–9. [PubMed: 12441146]
5. Wiesner J, Resemann A, Evans C, Suckau D, Jabs W. Advanced mass spectrometry workflows for analyzing disulfide bonds in biologics. Expert Rev. Proteomics. 2015; 12:115–123. [PubMed: 25720436]
6. Gorman JJ, Wallis TP, Pitt JJ. Protein disulfide bond determination by mass spectrometry. Mass Spectrom. Rev. 2002; 21:183–216. [PubMed: 12476442]
7. Foley SF, Sun Y, Zheng TS, Wen D. Picomole-level mapping of protein disulfides by mass spectrometry following partial reduction and alkylation. Anal. Biochem. 2008; 377:95–104. [PubMed: 18358819]
8. Chait BT. Mass Spectrometry: Bottom-Up or Top-Down? Science. 2006; 314:65–66. [PubMed: 17023639]
9. Doerr A. Top-down mass spectrometry. Nature Methods. 2008; 5:24–24.
10. Chen J, Shiyanov P, Zhang L, Schlager JJ, Green-Church KB. Top-Down Characterization of a Native Highly Intralinked Protein: Concurrent Cleavages of Disulfide and Protein Backbone Bonds. Anal. Chem. 2010; 82:6079–6089. [PubMed: 20560528]
11. Kleinnijenhuis AJ, Duursma MC, Breukink E, Heeren RMA, Heck AJR. Localization of Intramolecular Monosulfide Bridges in Lantibiotics Determined with Electron Capture Induced Dissociation. Anal. Chem. 2003; 75:3219–3225. [PubMed: 12964772]
12. Peng Y, Chen X, Sato T, Rankin SA, Tsuji RF, Ge Y. Purification and High-Resolution Top-Down Mass Spectrometric Characterization of Human Salivary α-Amylase. Anal. Chem. 2012; 84:3339–3346. [PubMed: 22390166]
13. Zubarev RA, Kelleher NL, McLafferty FW. Electron Capture Dissociation of Multiply Charged Protein Cations. A Nonergodic Process. J. Am. Chem. Soc. 1998; 120:3265–3266.
14. Kruger NA, Zubarev RA, Carpenter BK, Kelleher NL, Horn DM, McLafferty FW. Electron capture versus energetic dissociation of protein ions. Int. J. Mass Spectrom. 1999; 182–183:1–5.
15. Zubarev RA, Kruger NA, Fridriksson EK, Lewis MA, Horn DM, Carpenter BK, McLafferty FW. Electron Capture Dissociation of Gaseous Multiply-Charged Proteins Is Favored at Disulfide Bonds and Other Sites of High Hydrogen Atom Affinity. J. Am. Chem. Soc. 1999; 121:2857–2862.
16. Moore BN, Ly T, Julian RR. Radical conversion and migration in electron capture dissociation. J. Am. Chem. Soc. 2011; 133:6997–7006. [PubMed: 21495634]
17. Simons J. Mechanisms for S–S and N–Cα bond cleavage in peptide ECD and ETD mass spectrometry. Chem. Phys. Lett. 2010; 484:81–95.

18. Zhurov KO, Fornelli L, Wodrich MD, Laskay UA, Tsybin YO. Principles of electron capture and transfer dissociation mass spectrometry applied to peptide and protein structure analysis. Chem. Soc. Rev. 2013; 42:5014–5030. [PubMed: 23450212]
19. Syka JEP, Coon JJ, Schroeder MJ, Shabanowitz J, Hunt DF. Peptide and protein sequence analysis by electron transfer dissociation mass spectrometry. Proc. Natl. Acad. Sci. USA. 2004; 101:9528–9533. [PubMed: 15210983]
20. Cole SR, Ma X, Zhang X, Xia Y. Electron transfer dissociation (ETD) of peptides containing intrachain disulfide bonds. J. Am. Soc. Mass Spectrom. 2012; 23:310–320. [PubMed: 22161508]
21. Ni W, Lin M, Salinas P, Savickas P, Wu S-L, Karger B. Complete Mapping of a Cystine Knot and Nested Disulfides of Recombinant Human Arylsulfatase A by Multi-Enzyme Digestion and LC-MS Analysis Using CID and ETD. J. Am. Soc. Mass Spectrom. 2013; 24:125–133. [PubMed: 23208745]
22. Ganisl B, Breuker K. Does Electron Capture Dissociation Cleave Protein Disulfide Bonds? ChemistryOpen. 2012; 1:260–268.
23. Zhang Y, Cui W, Zhang H, Dewald HD, Chen H. Electrochemistry-Assisted Top-Down Characterization of Disulfide-Containing Proteins. Anal. Chem. 2012; 84:3838–3842. [PubMed: 22448817]
24. Zhang Y, Dewald HD, Chen H. Online Mass Spectrometric Analysis of Proteins/Peptides Following Electrolytic Cleavage of Disulfide Bonds. J. Proteome Res. 2011; 10:1293–1304. [PubMed: 21197958]
25. Nicolardi S, Giera M, Kooijman P, Kraj A, Chervet J-P, Deelder A, van der Burgt YM. On-Line Electrochemical Reduction of Disulfide Bonds: Improved FTICR-CID and -ETD Coverage of Oxytocin and Hepcidin. J. Am. Soc. Mass Spectrom. 2013; 24:1980–1987. [PubMed: 24018861]
26. Nicolardi S, Deelder AM, Palmblad M, van der Burgt YEM. Structural Analysis of an Intact Monoclonal Antibody by Online Electrochemical Reduction of Disulfide Bonds and Fourier Transform Ion Cyclotron Resonance Mass Spectrometry. Anal. Chem. 2014; 86:5376–5382. [PubMed: 24780057]
27. Mentinova M, McLuckey SA. Cleavage of multiple disulfide bonds in insulin via gold cationization and collision-induced dissociation. Int. J. Mass Spectrom. 2011; 308:133–136. [PubMed: 22125416]
28. Lee M, Lee Y, Kang M, Park H, Seong Y, June Sung B, Moon B, Bin Oh H. Disulfide bond cleavage in TEMPO-free radical initiated peptide sequencing mass spectrometry. J. Mass Spectrom. 2011; 46:830–839. [PubMed: 21834022]
29. Lomeli SH, Peng IX, Yin S, Ogorzalek Loo RR, Loo JA. New Reagents for Increasing ESI Multiple Charging of Proteins and Protein Complexes. J. Am. Soc. Mass Spectrom. 2010; 21:127–131. [PubMed: 19854660]
30. Yin S, Loo JA. Top-down mass spectrometry of supercharged native protein–ligand complexes. Int. J. Mass Spectrom. 2011; 300:118–122. [PubMed: 21499519]
31. Ogorzalek Loo RR, Lakshmanan R, Loo JA. What Protein Charging (and Supercharging) Reveal about the Mechanism of Electrospray Ionization. J. Am. Soc. Mass Spectrom. 2014; 25:1675–1693. [PubMed: 25135609]
32. Zhang J, Ogorzalek Loo RR, Loo JA. Increasing fragmentation of disulfide-bonded proteins for top–down mass spectrometry by supercharging. Int. J. Mass Spectrom. 2015; 377:546–556. [PubMed: 26028988]
33. Preiss JW, Setlow R. Spectra of Some Amino Acids, Peptides, Nucleic Acids, and Protein in the Vacuum Ultraviolet. J. Chem. Phys. 1956; 25:138–141.
34. Fung YM, Kjeldsen F, Silivra OA, Chan TW, Zubarev RA. Facile disulfide bond cleavage in gaseous peptide and protein cations by ultraviolet photodissociation at 157 nm. Angew. Chem. Int. Ed. 2005; 44:6399–6403.
35. Agarwal A, Diedrich JK, Julian RR. Direct elucidation of disulfide bond partners using ultraviolet photodissociation mass spectrometry. Anal. Chem. 2011; 83:6455–6458. [PubMed: 21797266]
36. Hendricks NG, Lareau NM, Stow SM, McLean JA, Julian RR. Bond-specific dissociation following excitation energy transfer for distance constraint determination in the gas phase. J. Am. Chem. Soc. 2014; 136:13363–13370. [PubMed: 25174489]

37. Zhang X, Li H, Moore B, Wongkongkathep P, Ogorzalek Loo RR, Loo JA, Julian RR. Radical-directed dissociation of peptides and proteins by infrared multiphoton dissociation and sustained off-resonance irradiation collision-induced dissociation with Fourier transform ion cyclotron resonance mass spectrometry. Rapid Commun. Mass Spectrom. 2014; 28:2729–2734. [PubMed: 25380495]
38. Chance RE, Ellis RM. Proinsulin: Single-chain precursor of insulin. Arch. Int. Med. 1969; 123:229–236. [PubMed: 4885673]
39. Loo JA, Edmonds CG, Smith RD. Primary sequence information from intact proteins by electrospray ionization tandem mass spectrometry. Science. 1990; 248:201–204. [PubMed: 2326633]
40. Henry KD, Williams ER, Wang BH, McLafferty FW, Shabanowitz J, Hunt DF. Fourier-transform mass spectrometry of large molecules by electrospray ionization. Proc. Natl. Acad. Sci. USA. 1989; 86:9075–9078. [PubMed: 2594751]
41. Przybylski M, Glocker MO. Electrospray Mass Spectrometry of Biomacromolecular Complexes with Noncovalent Interactions—New Analytical Perspectives for Supramolecular Chemistry and Molecular Recognition Processes. Angew. Chem. Int. Ed. 1996; 35:806–826.
42. Yu W, Vath JE, Huberty MC, Martin SA. Identification of the facile gas-phase cleavage of the Asp-Pro and Asp-Xxx peptide bonds in matrix-assisted laser desorption time-of-flight mass spectrometry. Anal. Chem. 1993; 65:3015–3023. [PubMed: 8256865]
43. Gardner M, Brodbelt J. Impact of proline and aspartic acid residues on the dissociation of intermolecularly crosslinked peptides. J. Am. Soc. Mass Spectrom. 2008; 19:344–357. [PubMed: 18083526]
44. Liu J, Gunawardena HP, Huang T-Y, McLuckey SA. Charge-dependent dissociation of insulin cations via ion/ion electron transfer. Int. J. Mass Spectrom. 2008; 276:160–170.
45. Tsybin YO, He H, Emmett MR, Hendrickson CL, Marshall AG. Ion Activation in Electron Capture Dissociation To Distinguish between N-Terminal and C-Terminal Product Ions. Anal. Chem. 2007; 79:7596–7602. [PubMed: 17874851]
46. Breuker K, Jin M, Han X, Jiang H, McLafferty FW. Top-Down Identification and Characterization of Biomolecules by Mass Spectrometry. J. Am. Soc. Mass Spectrom. 2008; 19:1045–1053. [PubMed: 18571936]
47. Lin C, Cournoyer JJ, O'Connor PB. Probing the Gas-Phase Folding Kinetics of Peptide Ions by IR Activated DR-ECD. J. Am. Soc. Mass Spectrom. 2008; 19:780–789. [PubMed: 18400512]
48. Mikhailov VA, Cooper HJ. Activated Ion Electron Capture Dissociation (AI ECD) of Proteins: Synchronization of Infrared and Electron Irradiation with Ion Magnetron Motion. J. Am. Soc. Mass Spectrom. 2009; 20:763–771. [PubMed: 19200749]
49. Rinker A, Halleman CD, Wedlock MR. Photodissociation dynamics of dimethyl disulfide. Chem. Phys. Lett. 2005; 414:505–508.
50. Stephansen AB, Brogaard RY, Kuhlman TS, Klein LB, Christensen JB, Sølling TI. Surprising Intrinsic Photostability of the Disulfide Bridge Common in Proteins. J. Am. Chem. Soc. 2012; 134:20279–20281. [PubMed: 23210550]
51. Stephansen AB, Larsen MAB, Klein LB, Sølling TI. On the photostability of the disulfide bond: An electronic or a structural property? Chem. Phys. 2014; 442:77–80.
52. Ly T, Julian RR. Ultraviolet Photodissociation: Developments towards Applications for Mass-Spectrometry-Based Proteomics. Angew. Chem. Int. Ed. 2009; 48:7130–7137.
53. Permyakov EA, Permyakov SE, Deikus GY, Morozova-Roche LA, Grishchenko VM, Kalinichenko LP, Uversky VN. Ultraviolet illumination-induced reduction of α-lactalbumin disulfide bridges. Proteins: Structure, Function, and Bioinformatics. 2003; 51:498–503.

Highlights

- UV (266-nm) activation can homolytically cleave a disulfide bond.
- UV-activation with ECD allowed the three disulfide bonds of insulin to be cleaved.
- For proteins, combined IR/UV-activation facilitates ECD disulfide bond cleavage.
- Protein S-S bonds can reform within 10–100 msec after their UV-homolytic cleavage.

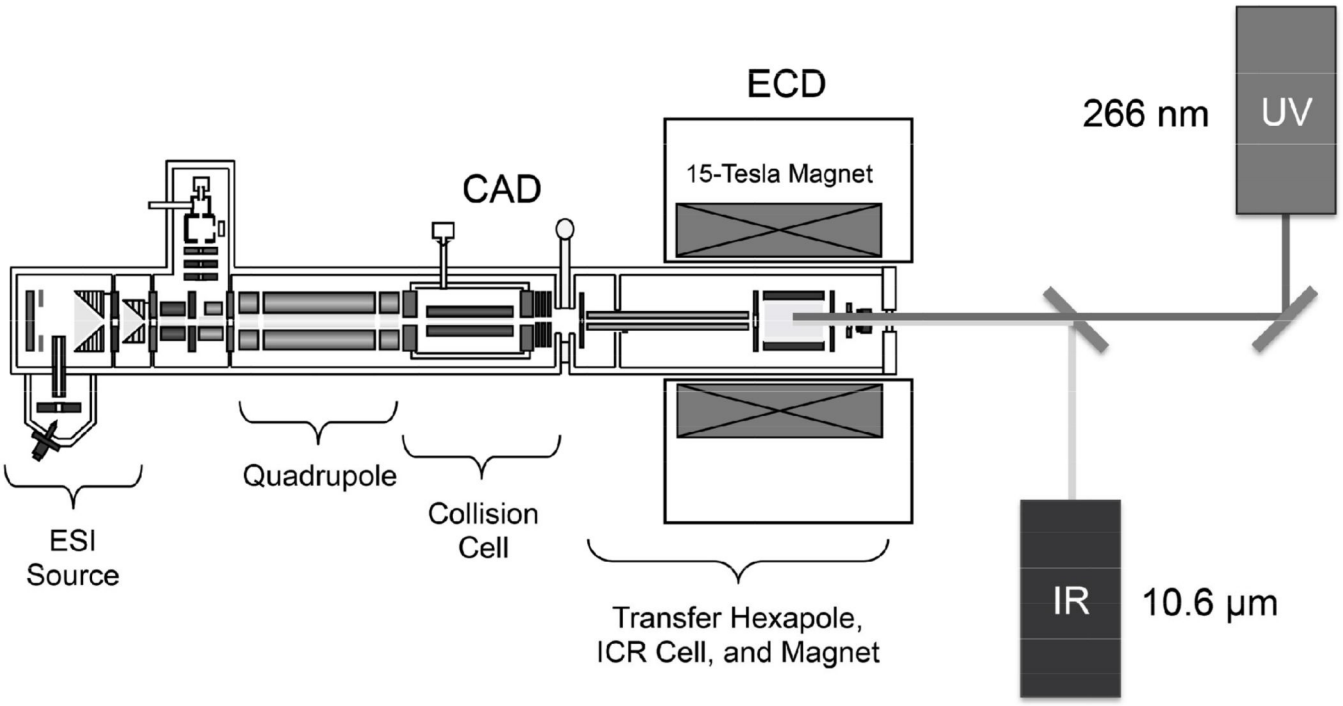

Figure 1.
Instrument diagram of the modified 15-Tesla FT-ICR mass spectrometer interfaced to the UV and IR lasers.

Figure 2.
Amino acid sequence and disulfide bonds of (a) bovine insulin and (b) bovine ribonuclease A.

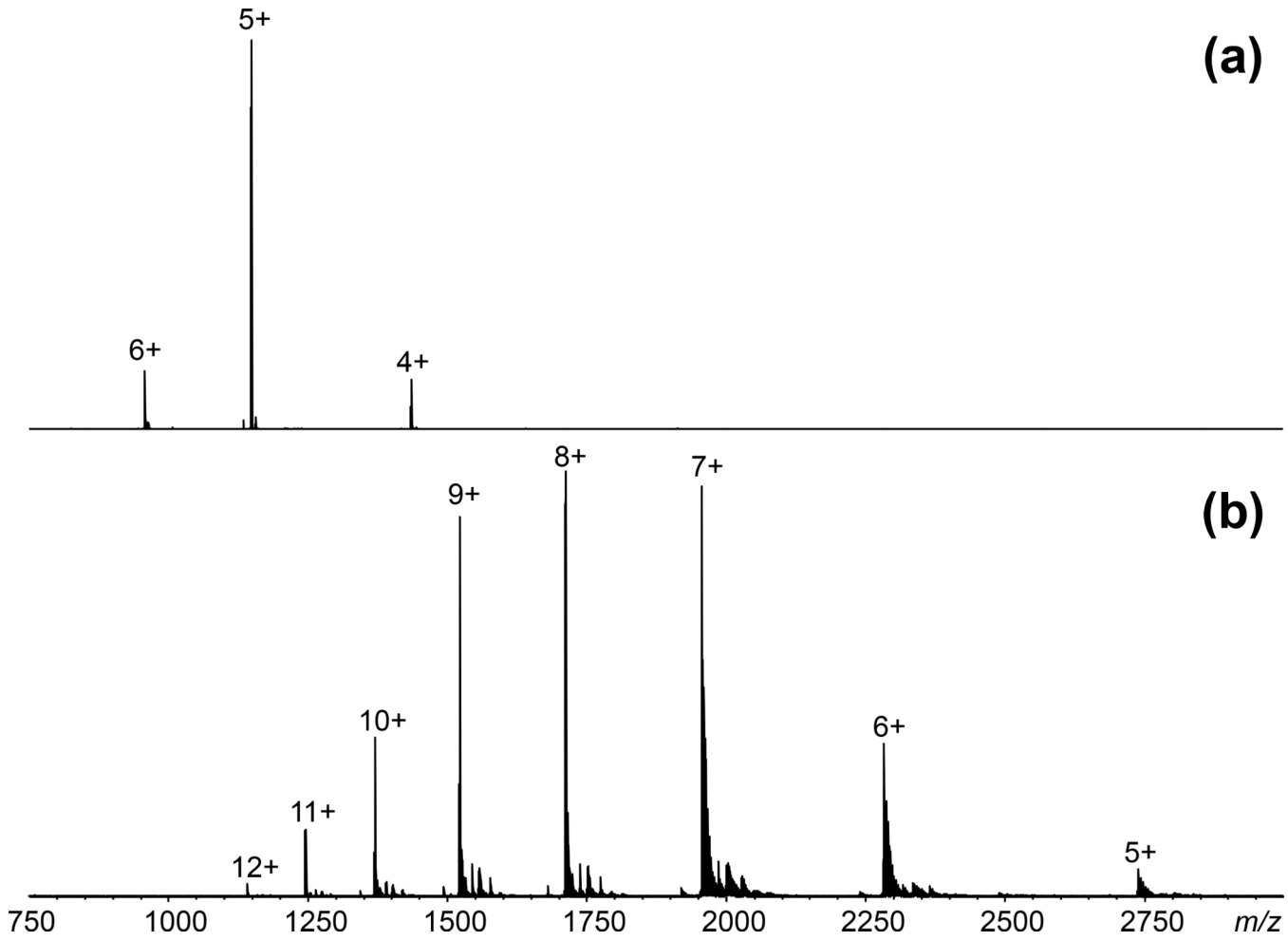

Figure 3.
ESI mass spectra of (a) insulin and (b) ribonuclease A.

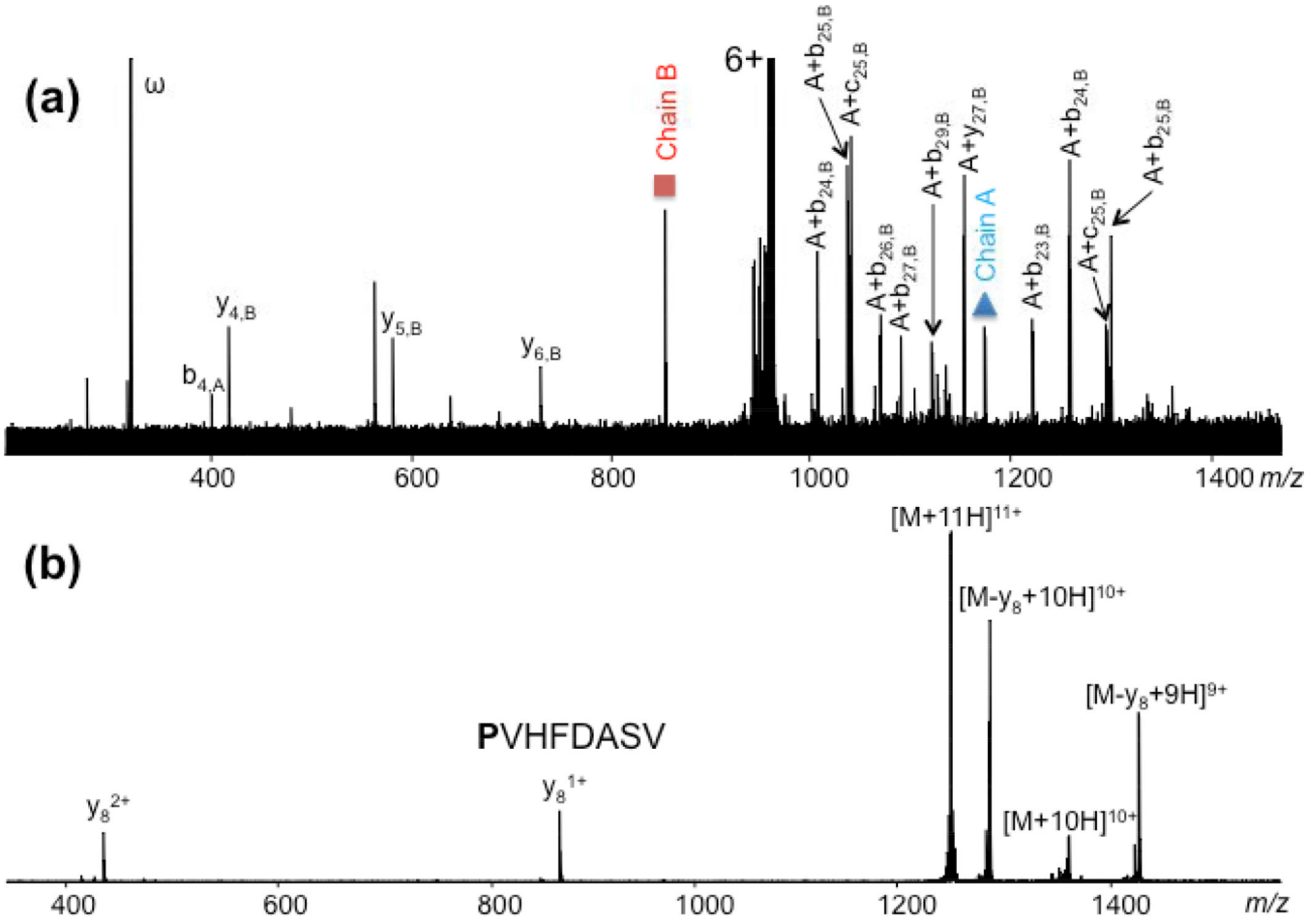

Figure 4.
UVPD (266 nm) mass spectra of (a) 6+ charged insulin and (b) 11+ charged ribonuclease A.

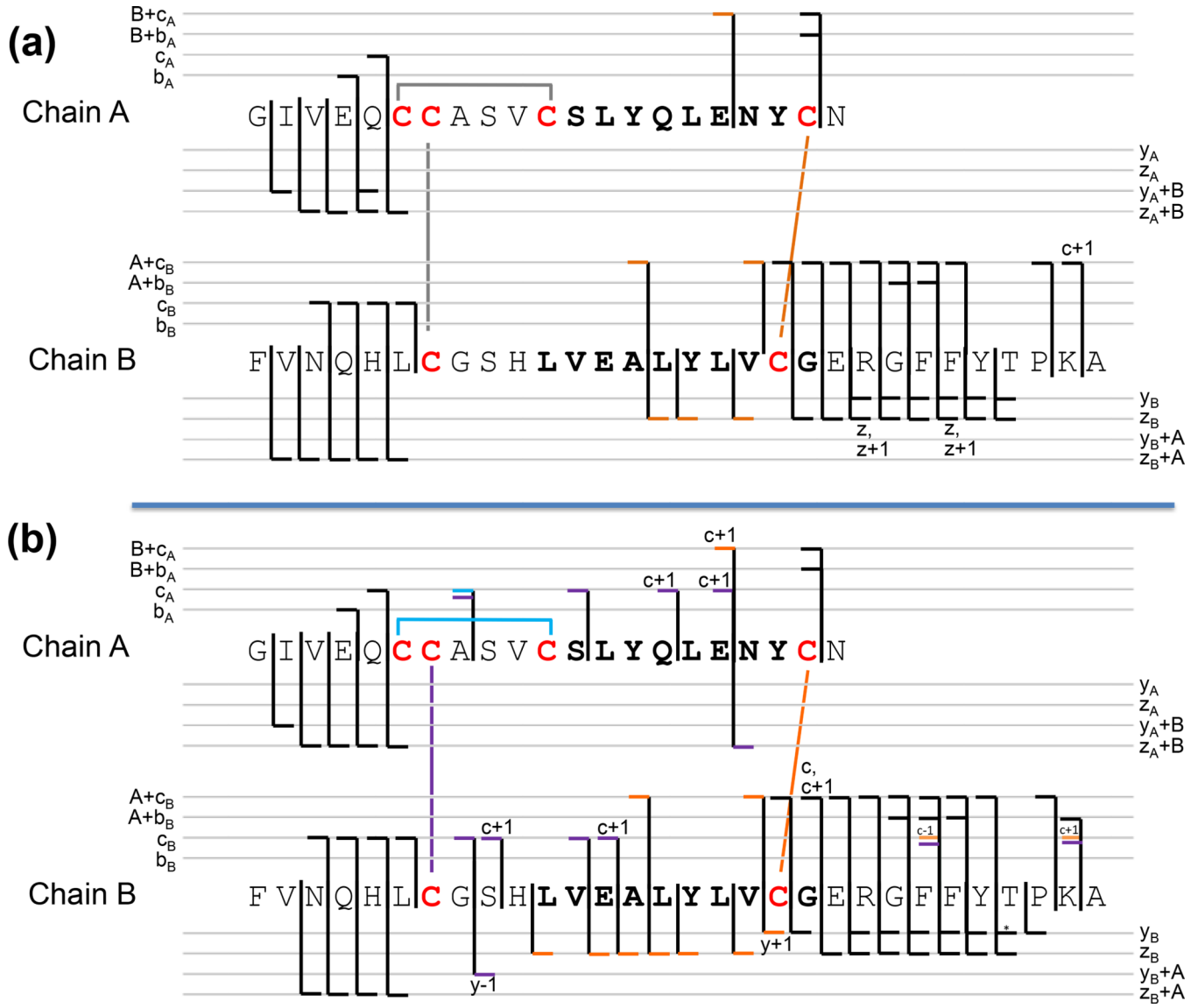

Figure 5.

Cleavage pattern of insulin by (a) ECD and (b) UV-activation/ECD showing one and three disulfide bonds cleaved, respectively. Fragments are color coded according to the corresponding cleaved disulfide bonds.

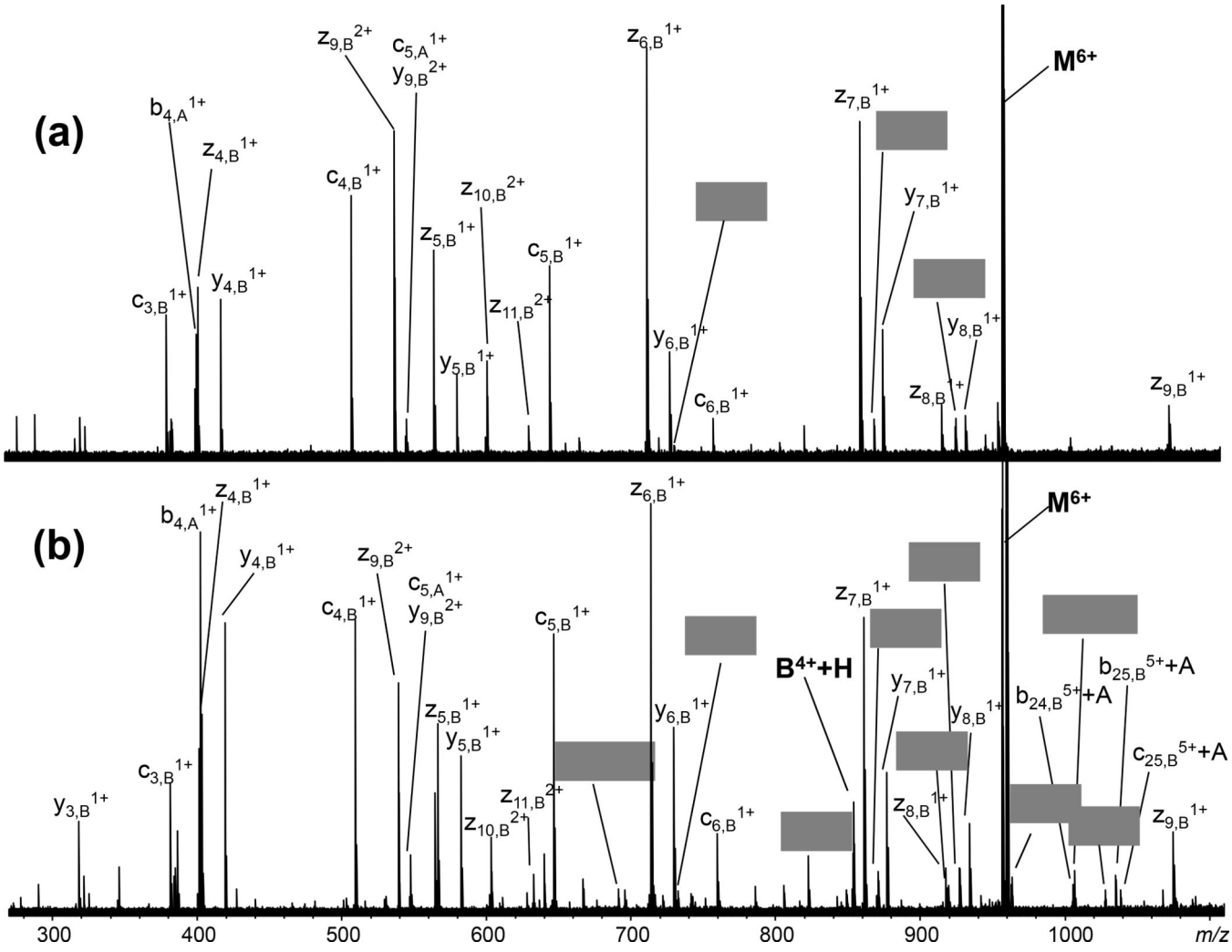

Figure 6.

Fragmentation mass spectra of 6+ charged insulin using (a) ECD and (b) UV-activation/ECD. Product ions confirming disulfide bond cleavages are highlighted with the boxed labels.

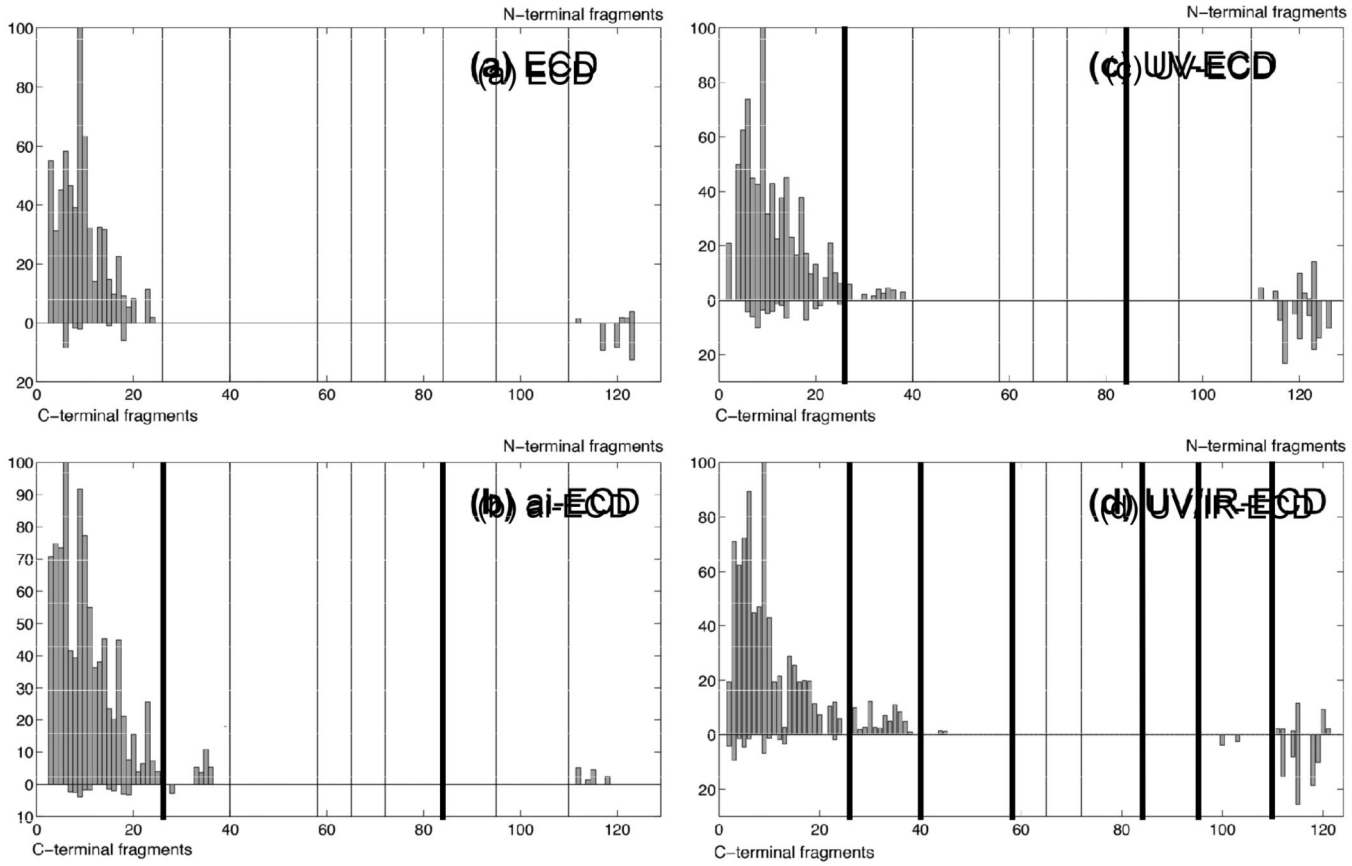

Figure 7.

Relative abundances of backbone fragmentation for ribonuclease A using (a) ECD, (b) ai-ECD, (c) UV-ECD, and (d) UV/IR-ECD. The vertical lines represent cysteine residues that form disulfide bonds. The bolded vertical lines indicate the cysteines where the disulfide bond cleavage occurred. Bars above the zero level represent N-terminal containing product ions (b- and c-products) and the bars below the zero level represent C-terminal containing product ions (y- and z-products).

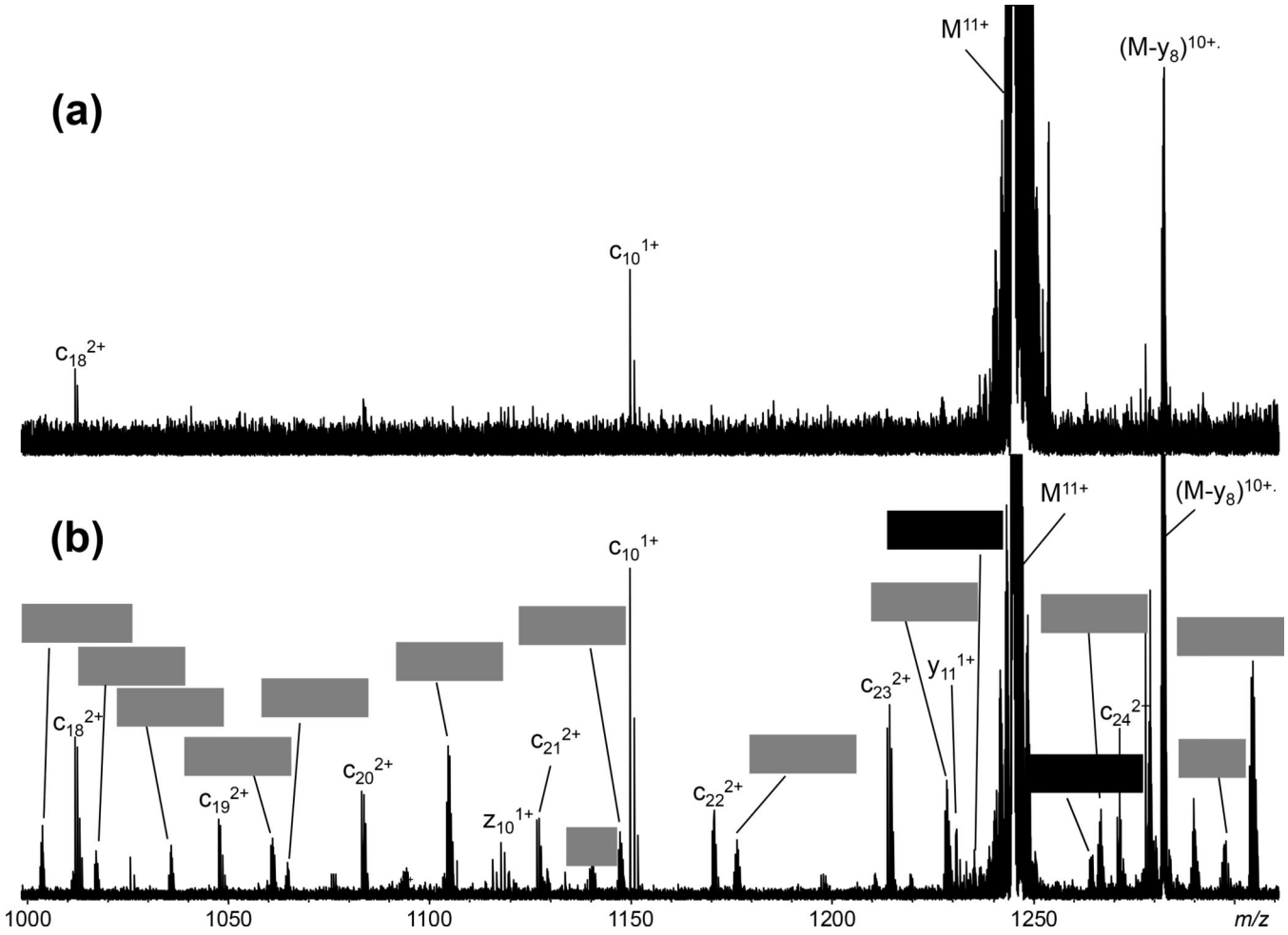

Figure 8.

(a) ECD mass spectra of the 11+ charged ribonuclease A and (b) with UV/IR- activation prior to ECD. Fragments from disulfide bridged regions are highlighted with the boxed labels.

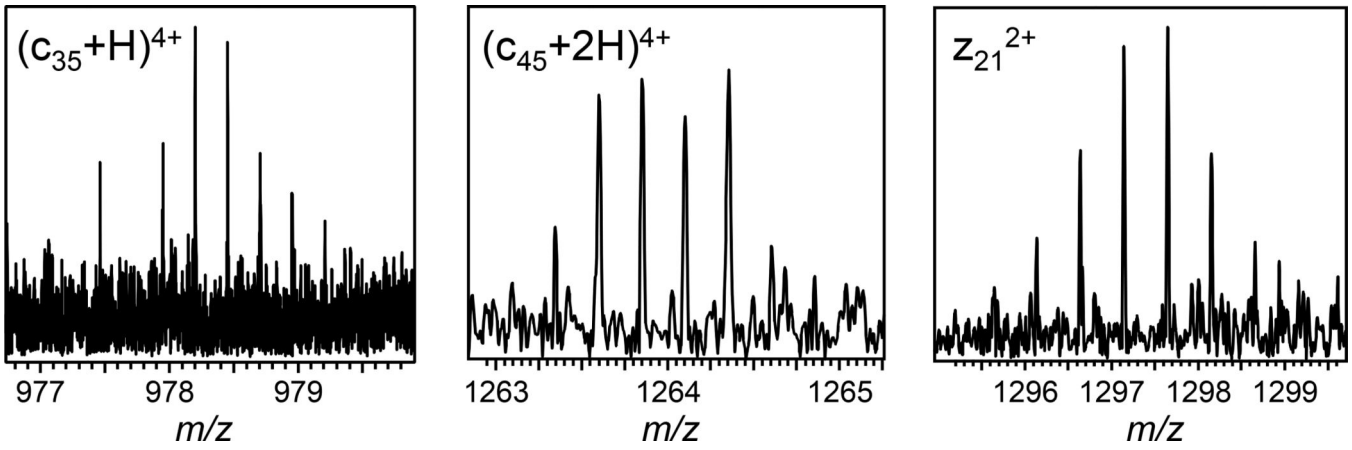

Figure 9.

UV/IR-activated ECD products (c_{35}+H, c_{45}+2H, and z_{21}) represent cleavage of the first, second, and third disulfide bonds, respectively, from ribonuclease A.

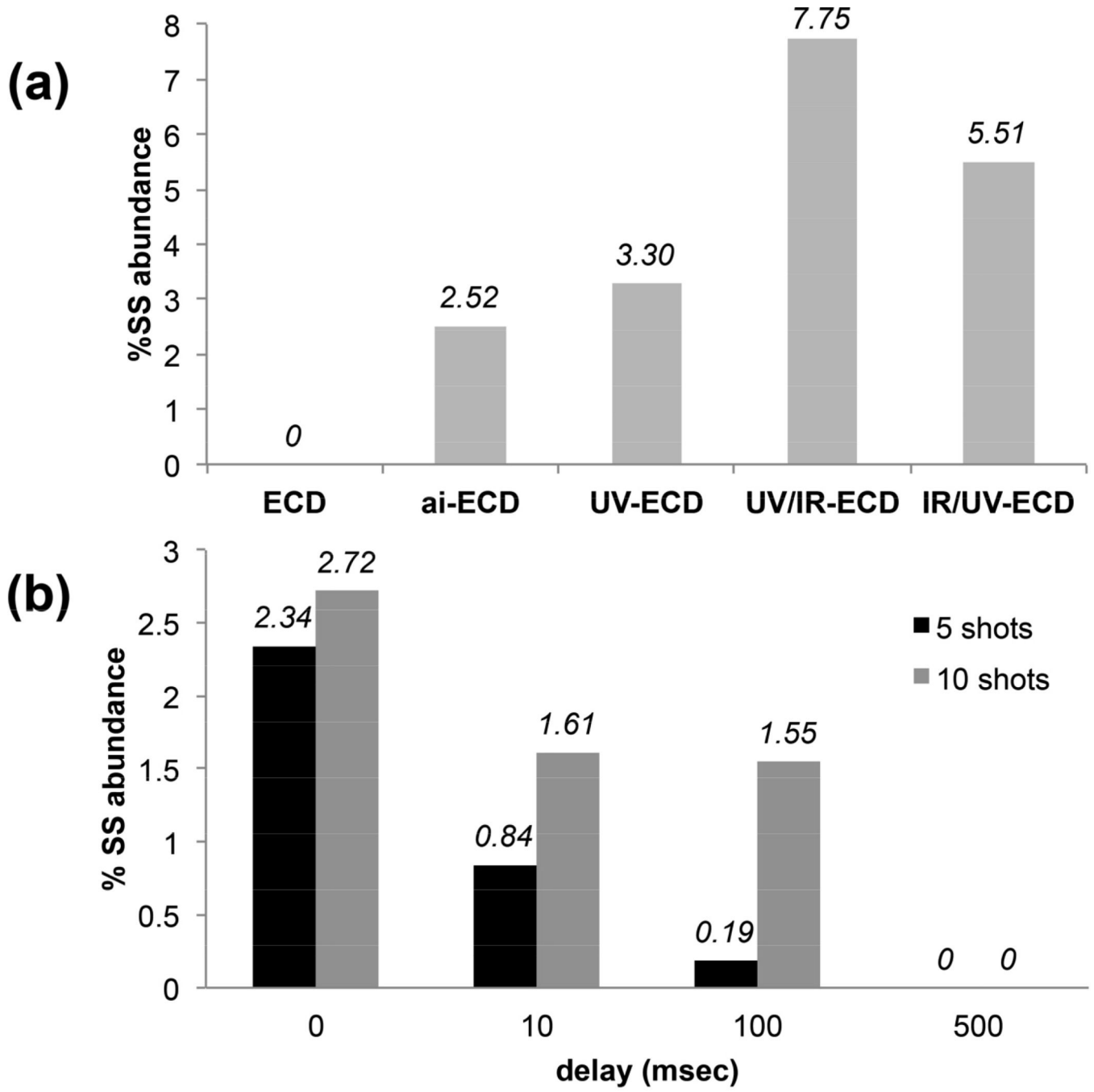

Figure 10.

Comparison of %SS abundance for ECD of ribonuclease A (a) between different activation conditions and (b) as a function of delay time between UV-activation and the ECD event for UV-ECD.